Journal of Fundamental and Applied Sciences

ISSN 1112-9867

Available online at http://www.jfas.info

Research Article

NUMERICAL STUDY ON THE IMPORTANCE OF THE MIXED CONVECTION AND THE IMPACT OF THE COOLING RATE ON THE SOLIDIFICATION OF A PURE MATERIAL

T. Bouzennada*, F. Mechighel

LR3MI Laboratory, Department of mechanical engineering, Faculty of engineering sciences, BP.12, Annaba University, Annaba, Algeria

Received: 08 August 2019 / Accepted: 29 August 2019 / Published online: 01 September 2019

ABSTRACT

The present paper investigates numerically the solidification process of a pure metal, injected inside a channel, aiming to overview theoretically this complex phase change process, using COMSOL Multiphysics. The study is based on the Voller and Prakash model with fixed grid technique [1]. Results interpretation have been steered toward guessing the effect on the whole process of a **varying entrance melt velocity**; having proven that melt flow has a *negative* effect on the solidification rate. Also, the **decreasing mid values of temperature transition** (MVTT) would give fine numerical solution because it offers less thick mushy zone; this allows a good understanding to the solidification rate, mushy zone spreading and flow structure nearby solid region. Then, **two different variable cooling rates** functions were suggested comparing them to constant heat flux case. Results indicate that *linear* function cooling heat flux is the best function in terms of economy of cooling costs.

Keywords: Solidification, Mushy zone, Melt flow, Free convection, Forced convection.

Author Correspondence, e-mail: tarek.bouzennada@univ-annaba.org

doi: http://dx.doi.org/10.4314/jfas.v11i3.10

1. INTRODUCTION

Solidification intervenes in many actual industrial applications nowadays. In fact, many particular processes are based on it, such as continuous casting [2, 3], crystal growth and welding [4, 5]. Thus various researches topics are on the solidification and its peripheral related issues in order to bring solution to its well common ordinary technical problems, which affect the quality of the final product. In general, solidification can be hardly malfunctioned due to the convective motions that could be occured in the melt (i.e. convective melt flows). It has been found that the strength of these melt flows causes a decline in solidification rate because of the *remelting* process. Especially in continuous casting applications (using pure metals to produce alloys) which are exploited in manufacturing metals frames. Engineering has brought many techniques to avoid inevitable processing issues such as controlled cooling rate and casting rate.

Many previous works focused on the cooling rate in extracting heat during a solidification of a steel metal inside a mold. For instance, Sengupta et al. [6] compared and discussed the effect of water cooling techniques which used for casting process of both steel and aluminum on the final product quality where the appearance of cracks due to a strong variation in temperature gradient were characterized. Elliott et al. [7] carried out an investigation aiming to establish a comparison between the effect of both cooling techniques “liquid-metal cooling (LMC)” and “conventional radiation cooling” during casting. In the first technique a solidification rate in the range of (2.5-8.5 mm/min) has been identified, and in the second one a casting rate of 2.5 mm/min has been chosen. Results showed that LMC technique provides higher thermal graduation due to a refined structure measurable by the finer dendrite-arm spacing. As for the conventional radiation cooling technique, some cracks and cavities (voids) appeared in the product, although none of these cracks had appeared while using LMC technique. Duan et al. [8] set a numerical study on pure metal solidification, filling a rectangular cavity and discussed the influence of the cold wall temperature condition and the aspect ratio on the solidification rate. It has been proven that there is no apparent effect of the aspect ratio on solidification rate. On the other hand, results show that the solid fraction increases if the temperature of the cold wall drops. Hameed et al. [4] led an investigation to

study both of primary and secondary cooling impact on continuous casting process of a copper made billet with fixing casting rate value. The results presented good quality in the final product with fewer losses due to extrusion found by controlling heat flux during the process.

Other studies were carried out to find causes and solution to the current casting issues such as gaps and metal malformations in the final product (see for instance [9]); however, computational numerical simulation has contributed significantly in predicting possible defects appearing during advanced stages of the solidification process and how to find methods to avoid it. Rao et al. [10] had reviewed details on proCast, a finite element method (FEM) based computer code to simulate solidification and casting in foundries. They found that foundries could derive mileage by resorting to FEM simulations of the casting process for process development and optimization. Many experimental studies were set to investigate casting rate effect on continuous casting process as Zhang et al. [11] applied different casting rates; the final results proved that several defects appear within the final product due to high casting rate injected in the mold. Mahmoudi and Fredriksson [12] conducted a numerical study with an experimental approach of continuous casting process, using the copper as pure metal. Results indicate that the solidification rate intensifies with respect to fasting casting rate, and the temperature gradation develops more as the casting rate goes higher, the thing that pushes faster the solidification rate. Also, Wu et al. [13] proved the negative effect of the remelting on the solidification, where the already solidified spots start to remelt due to the injected melt.

The present study focuses on the impact of mid value of transition temperature MVTT on the numerical results, and the flow rate of the molten metal (melt) that injected inside a channel (mold), and reviewing their effect on the solidification rate, structure of the melt flow, and both velocity and temperature field. The last part of this paper discusses a comparison between three cases each marked by its own cooling rate method. The aim is to investigate both the solidifcation rate and the cooling heat flux in each case to economise the energy.

2. GENERAL CONSIDERATIONS AND MATHEMATICAL MODEL

Consider the solidification of the molten copper filled in a channel as shown in Fig.1. The channel is subjected to the boundary conditions shown in the figure. The thermo-physical properties of copper (solid and liquid) are collected from [14] and shown in the table 1.

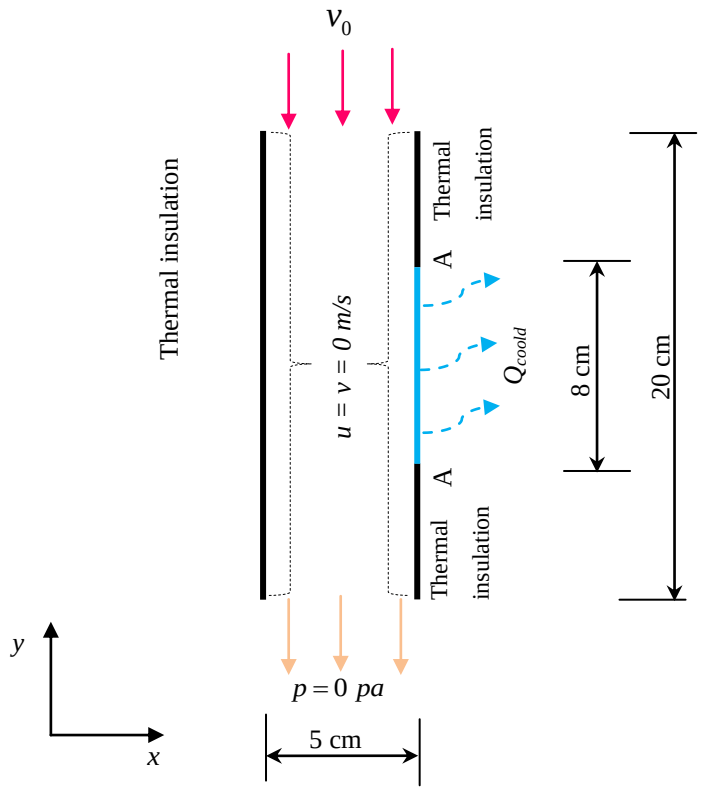

Fig.1. Presentation of the physical problem

This study proposes the Voller and Prakash model [1] combined with the heat and momentum transports equations, written in its general form as suggested by Patankar [15] as mean to model and solve metal solidification process and both heat and flow problem, respectively.

In its basic consideration, Voller and Prakash's model presents the physical domain shown in Fig.1 as a *porous* medium with a porosity designated by, ε_l .

Remark 1: In the present study, since it was assumed that for the copper $\rho_l = \rho_s$ (see the table 1 below) thus the porosity (i.e. liquid volume fraction) of the porous medium, ε_l ,

should be taken identical to the liquid fraction f_l (i.e. $\varepsilon_l = f_l = 1 - f_s$)). It takes the values, $\varepsilon_l = f_l = 1$ in the liquid phase, $\varepsilon_l = f_l = 0$ in the solid and $0 < (\varepsilon_l = f_l) < 1$ in the mushy zone.

Table 1. Thermo-physical properties of the copper (solid and liquid) used in the present numerical computations [14]

Thermo-physical properties	**Liquid (melt)**	**Solid**
Density, ρ [kg/m^3]	8933	8933
Specific heat, c_p [J/kg K]	531*	385
Thermal conductivity, k [W/m K]	401	401
Viscosity, μ [N s/m^2]	0.0434	-
Thermal expansion coefficient β [K^{-1}]	16.5 10^{-6}	-

Other input parameters includes: latent heat of fusion, $L_f = 205$ kJ/kg, melting temperature, $T_m = 1358$ K, and initial melt temperature, $T_{in} = 1473$K.

*Instead using this value, the liquid specific heat used in the present study is predicted from the Eqution (16) below.

In addition, in above model the solution of the heat transport problem is an enthalpy-based numerical tool given as:

$$H = h + \Delta H = c_p T + f(T) \quad (1)$$

where H is the total enthalpy (specific quantity). In the equation (1), the *sensible* heat (enthalpy), *h*, during the process is assumed to be $h = c_p T$ (where c_p is the specific heat of the medium) and the mushy magnitude of the disturbance and resulting mixing in the advanced stages of the solidification process zone's change requires that the *latent* heat contribution, ΔH, may be specified as a *function* of temperature, *T*, such as $\Delta H = f(T)$. The latent heat of phase change may be also defined as a function of the liquid fraction within the porous medium such as: $\Delta H = f(T) = f_l L_f = f_l(T) L_f$, where L_f represents the latent heat of fusion of the material (a given value for the chosen material, see the table 1).

On the other hand, in the porous medium, the liquid mass fraction f_l of the material (copper) varies with the temperature, *T*, and may be expressed as:

$$f_l = f_l(T) = 1 - f_s(T) = \begin{cases} 1 & \text{if} \quad T > T_l \\ f_l & \text{if} \quad T_l > T \geq T_s \\ 0 & \text{if} \quad T < T_s \end{cases} \tag{2a}$$

which may be written as

$$f_l(T) = 1 - f_s(T) = \begin{cases} 1 & \text{if} \quad T > T_l \\ \dfrac{(T - T_s)}{(T_l - T_s)} & \text{if} \quad T_s < T \leq T_l \\ 0 & \text{if} \quad T < T_s \end{cases} \tag{2b}$$

where T_l represents the temperature of the melt at the starting point of the solidification, T_s is the temperature of solid at the end of the solidification process, and f_s is the solid mass fraction.

The equation (2b) can be expressed in terms of the melting temperature, T_m, such as:

$$f_l(T) = 1 - f_s(T) = \begin{cases} 1 & \text{if} \quad T > T_m + dT \\ \dfrac{[T - (T_m + dT)]}{2dT} & \text{if} \quad (T_m - dT) < T \leq (T_m + dT) \\ 0 & \text{if} \quad T < T_m - dT \end{cases} \tag{3}$$

The expression (3) is the *linear* form of f_l based on the Voller and Prakash model [1], where $T_s = T_m - dT$, $T_l = T_m + dT$ and dT is the mid value of the temperature transition (with $dT = (T_l - T_s)/2$). In a simplified form, the above expression can be written as:

$$f_l(T) = 1 - f_s(T) = \begin{cases} 1 & \text{if} \quad T > T_l \\ \dfrac{T - T_l}{2\,dT} & \text{if} \quad T_s \leq T \leq T \\ 0 & \text{if} \quad T < T_s \end{cases} \tag{4}$$

2.1 Governing Equations

For the physical problem shown in Fig.1 and assumed as a porous medium, the hydrodynamic equations can be written in terms of *superficial* velocity (i.e. the mean velocity of the system), which reads

$$\mathbf{u} = \varepsilon_l \mathbf{u}_l = f_l \mathbf{u}_l \tag{5}$$

where $\mathbf{u}_l$ is the *actual* velocity in the liquid (velocity in the liquid phase). From the

expression, $\varepsilon_l = f_l = 1 - f_s$, the equation (5) can be extended to

$$\mathbf{u} = \begin{cases} \mathbf{u}_l, & \text{in the liquid phase} \\ f_l \mathbf{u}_l, & \text{in the mushy zone} \\ 0, & \text{in the solid phase} \end{cases} \quad (6)$$

By using this definition and assuming a laminar flow of an incompressible and Newtonian fluid (melt). Governing equations for the physical problem, shown in Fig.1, are:

Conservation of mass

$$\frac{\partial u}{\partial x} + \frac{\partial v}{\partial y} = 0 \quad (7)$$

Conservation of momentum

$$\frac{\partial \rho u}{\partial t} + u\frac{\partial \rho u}{\partial x} + v\frac{\partial \rho u}{\partial y} = -\frac{\partial p}{\partial x} + \mu\left[\frac{\partial^2 u}{\partial x^2} + \frac{\partial^2 u}{\partial y^2}\right] + F_x \quad (8a)$$

$$\frac{\partial \rho v}{\partial t} + u\frac{\partial \rho v}{\partial x} + v\frac{\partial \rho v}{\partial y} = -\frac{\partial p}{\partial y} + \mu\left[\frac{\partial^2 v}{\partial x^2} + \frac{\partial^2 v}{\partial y^2}\right] + F_y + F_g \quad (8b)$$

where u and v are the superficial velocities in the vertical and horizontal directions, respectively. ρ is the density, p represents the pressure and μ is the liquid viscosity (see the table 1). In the equations (8a) and (8b), F_x, F_y and F_g represent the source terms which could be illustrated as follows:

Expressions for the Source Terms F_x **and** F_y

For a porous medium, the flow inside the mushy zone is assumed to be governed by the *Darcy* law:

$$\mathbf{u} = -(\kappa/\mu)\nabla p = -(\kappa/\mu)\left(\frac{\partial p}{\partial x}\mathbf{e}_x + \frac{\partial p}{\partial y}\mathbf{e}_y\right) \quad (9)$$

where κ is the permeability of the mushy zone.

As mentioned before the function of the porosity ε_l is given as $\varepsilon_l = f_l = 1 - f_s$, thus if the porosity decreases both the superficial velocity and the permeability decrease as well. This decrement could be downing into a zero value once the mushy zone is entirely solid ($\varepsilon_l = 0$) and the source terms (F_x and F_y in the momentum conservation equations) are given as:

$$F_x = \mathcal{A} u \quad \text{and} \quad F_y = \mathcal{A} v \tag{10}$$

where $\mathcal{A}$ is a function referred to each zone of the phase change (liquid, mushy zone or solid). Following the value of the function $\mathcal{A}$ one can distinguish the following cases: If $0 < \mathcal{A} < 1$ the equations of dynamics are close to the Darcy law (mushy (porous) region); if $\mathcal{A} = 0$, which involves that $F_x = 0$ and $F_y = 0$, in this case the velocities are actual which means the nonexistence of any form of porous medium (liquid zone) and finally the case where $\mathcal{A} = 1$ which means that all the equation terms are close to zero (solid phase). The expression of the function $\mathcal{A}$ may be derived from the Kosney-Carman equation [16]:

$$\mathcal{A} = -C\left(1-\varepsilon_l\right)^2 \Big/ \left(\varepsilon_l^3 + q\right) \tag{11}$$

where the value of the parameter *C* depends on the *morphology* of the porous medium; the value $C = 10^6$ kg/m^{3}s (constant value taken form [17]) is used in the present study, and q is a constant used to avoid floating error or division by zero (in the present predictions q is chosen to be 0.001).

Expressions for the Source Term F_g

The channel full of molten metal (copper melt), is exposed to high temperature and being cooled using cold source; thus the liquid metal is in movement due to changing in melt density; this phenomenon is driven by buoyancy force for natural convection, defined by the source term F_g as following

$$F_g = \rho \beta g (T - T_m) \tag{12}$$

where β is the thermal expansion coefficient of the copper liquid (see the table 1) and g represents the gravity.

Energy equation

For the physical problem, shown in Fig.1, the energy equation may be expressed in terms of the sensible enthalpy such as:

$$\frac{\partial \rho h}{\partial t} + u\frac{\partial \rho h}{\partial x} + v\frac{\partial \rho h}{\partial y} = \frac{k}{c_p}\left[\frac{\partial^2 h}{\partial x^2} + \frac{\partial^2 h}{\partial y^2}\right] - S_h \tag{13}$$

where S_h represents the source term for the energy conservation equation (13). This term is given as

$$S_h = \frac{\partial(\rho \Delta H)}{\partial t} + \nabla \cdot (\rho \mathbf{u} \Delta H) = \frac{\partial(\rho \Delta H)}{\partial t} + \mathbf{u} \cdot \nabla(\rho \Delta H) \quad (14)$$

This expression is derived from the enthalpy formula for the convection-diffusion phase change problem [18]. In a Cartesian coordinate system, the projection of the equation (14) leads to

$$S_h = \frac{\partial(\rho \Delta H)}{\partial t} + u\frac{\partial(\rho \Delta H)}{\partial x} + v\frac{\partial(\rho \Delta H)}{\partial y} \quad (15)$$

Recall that the total enthalpy, H, is defined as $H = c_p T + \Delta H = c_p T + f_l L_f$ (see Eq. (1)).

Remark 2*:* here using $\rho_l = \rho_s = \rho$ and $k_l = k_s = k$, where ρ_l and k_l represent the density and thermal conductivity of liquid, respectively; ρ_s and k_s the density and thermal conductivity of solid.

Expressions for the Specific Heat at Constant Pressure "c_p"

During the solidification process the melt is progressively cooled inside the channel, and thus a significant quantity of heat (latent heat of phase change) is released. Mainly, the specific heat c_p is admitted to be a function of the temperature during the process [19], such as:

$$c_p = c_{ps} + \Delta H\left(\frac{1}{T_m H} + \eta\right) \quad (16)$$

where c_{ps} is the value of specific heat of the solid phase (see the table 1) and η is a temperature-dependence expression which may be picked out from the Gaussian curve and given by $\eta = e^{\left(-(T-T_m)^2/dT^2\right)} \Big/ \left(dT\sqrt{\pi}\right)$.

2.2. Initial and Boundary Conditions

The present study is conducted within an open channel (with $5\text{cm} \times 20\text{cm}$, see Fig.1) in order to allow the melt flow passing through it, and the melt is being cooled to solidify by applying a cold heat flux originated from the middle section of the channel's left wall of 8 cm side (section A-A, see Fig.1).

The non-slip boundary condition is applied for the velocity which implies that $u = v = 0$ m/s on all the surfaces of the channel except the inlet and outlet sections where the entrance velocity is set as v_0 on the channel entrance (inlet section) and the pressure is set to be zero at the channel outlet (outlet section).

The thermally insulated boundary condition is applied for the temperature on all the surfaces of the channel except for the inlet section where the temperature is set to be T_{in} = 1473 K and a set cooled flux as $Q_{cooled} = -8\times10^5 \ \mathrm{W/m^2}$ on the section A-A of the left wall (cooled part) (see Fig.1).

The values $T = T_{in} = 1473K$ and $\mathbf{u} = \mathbf{0}$ (i.e. $u = v = 0 \ \mathrm{m/s}$) are taken as initial values for the temperature and velocity, respectively.

3. RESULTS AND DISCUSSION

Meshing and Numerical Resolution

Problems of phase change during convection that based on momentum and energy transport equations are extremely complicated nonlinear sort of problem. Accordingly it is hard to find coherent numerical solution in simple fast way. So, choosing the computation grid is essential for suitable numerical solution.

The criterion to choose an appropriate grid is based on its resolution and the computation cost. Grid offering less computation time with fine results has been chosen (solid fraction average). The actual grid is selected among shown grids in Fig. 2, and it consists of **5425** domain elements and 233 boundary elements.

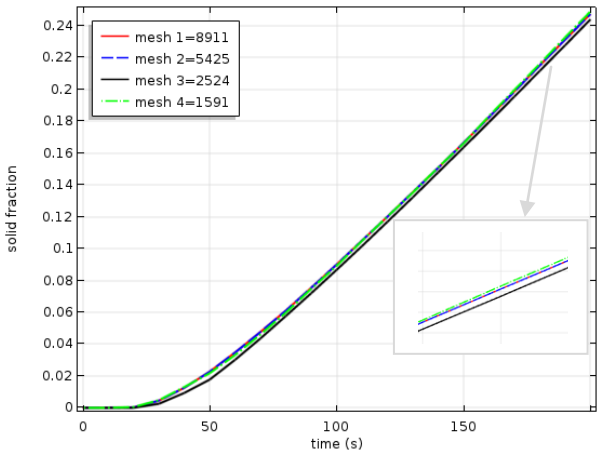

Fig.2. Mesh element size (predictions performed with $v_0 = 0.001 \ \mathrm{m/s}$ and $dT = 5K$).

COMSOL multiphysics environment [20] is the numerical tool involving to solve the present

problem. Fig. 3 shows the shape of the computation grid used to divide the physical domain of the problem. A complete refining in whole domain is made to adapt to the moving mushy zone and to cover up the time dependent developing velocity and temperature fields.

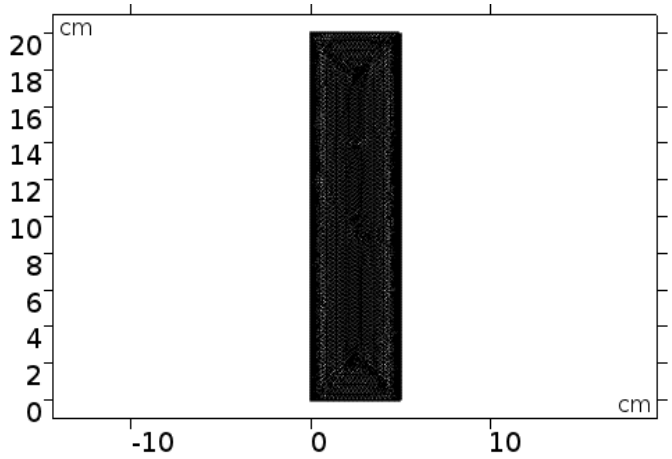

Fig.3. Computation grid used in the present simulations.

3.1 Velocity Filed

The velocity begins in an initial value v_0, set to be $v_0 = 0.001\,\mathrm{m/s}$ in these results. The flow penetrates the channel, and as time goes, the value of the velocity rises right at the middle area of the channel due to the decreasing of the passage section in time; hence the narrowing melt passage section is due to the partial solidification of the melt from the right wall toward the left, and the velocity takes maximum value in axial region of the gradation of the velocity. The mass conservation law is verified as shown in Fig. 4 at different time steps (t = 20, 50, 100 and 200 s).

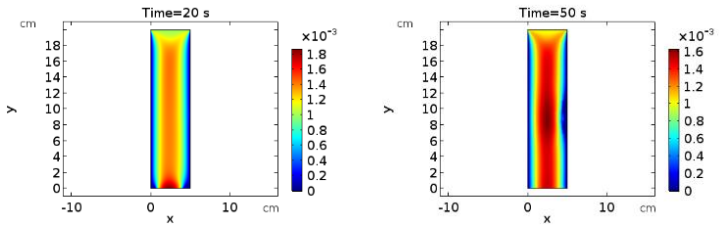

(a) (b)

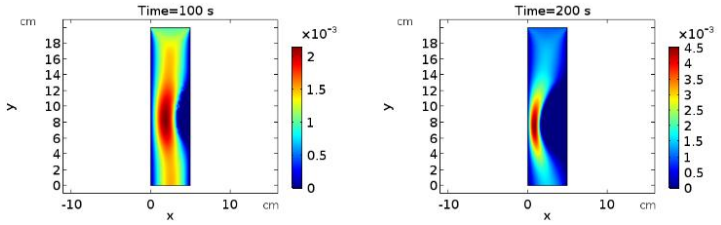

(c) (d)

Fig.4. Velocity field at different time steps ($v_0 = 0.001\,\mathrm{m/s}$ and $dT = 5K$).

3.2 Temperature filed

Fig. 5 presents the isotherms at different time steps (t = 20, 50, 100 and 200 s). It is shown that the temperature decreases from cooled region toward the center of the channel in time's advance; as well, it can be said here that the isothermal lines (isotherms) take a curvy shaped form beginning from cooled part toward the inner part of the channel.

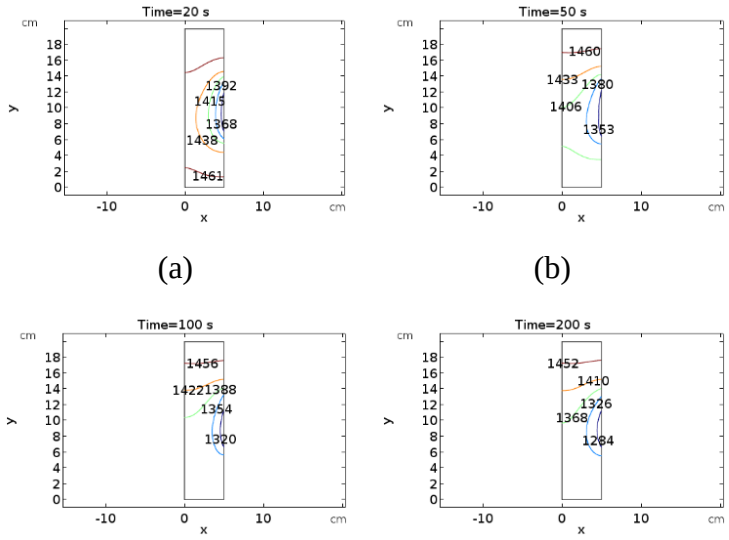

(a) (b)

(c) (d)

Fig.5. Isotherms at different time steps ($v_0 = 0.001\,\mathrm{m/s}$ and $dT = 5K$).

3.3 Solid Fraction, Mushy Zone and Flow Structure

The results in Fig. 6 show the solid fraction development and the structure of the melt flow at different time steps (t = 20, 50, 100 and 200 s), where the solidification started from cooled region and spread in time into the middle area of the channel. The solid part is taking a curved shape. In addition, the structure of the flow changes with the changing occurring in the solid

part. The streamlines do not pass over the part that has solidified matching exactly what is shown in the results.

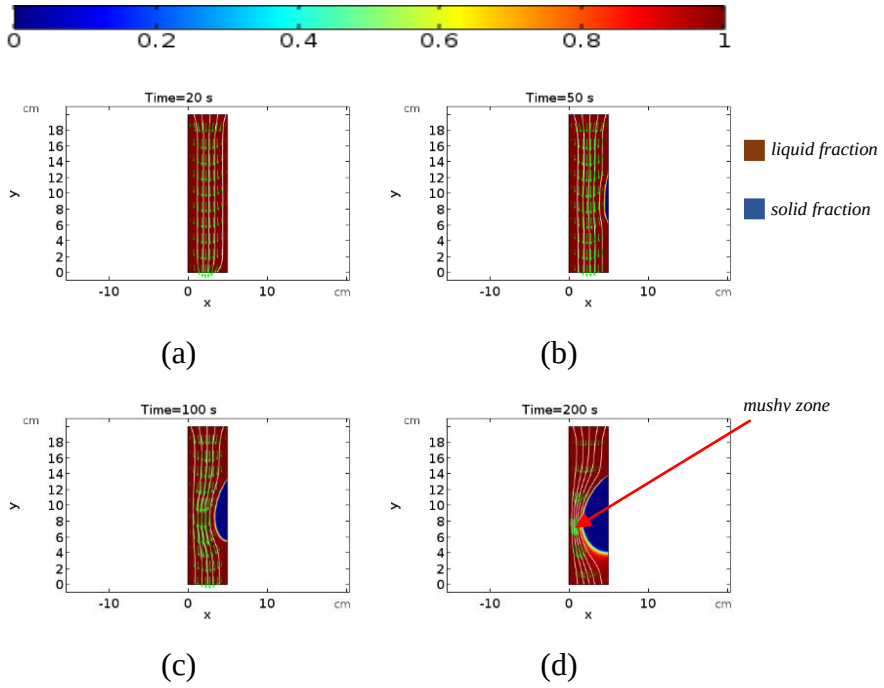

Fig.6. Solid fraction and flow structure at different time steps ($v_0 = 0.001\,\mathrm{m/s}$ and $dT = 5K$)

3.4 Effect of Mid Values of Temperature Transition (MVTT)

3.4.1 Velocity Filed

Fig. 7 gives the results of the impact related to variable MVTT values on the velocity fields; this impact is set to be inspected at unique time step (200 s). According to the results there is no observed effect on velocity field formation that could be related to variable MVTT values.

3.4.2 Temperature Filed

Isotherms are presented in Fig. 8 at unique time step (200 s); investigating the effect of MVTT value on it, results show its unclear weak influence on the formation of the temperature field during the process.

3.4.3 Solid Fraction, Mushy Zone and Flow Structure

Fig. 9 shows the solid fraction development while changing MVTT values at a unique time step (200 s). Observation indicates that as long as the values of MVTT decrease the mushy zone gets less thick as well, although, the computation taken time got longer at each single case. As conclusion, it is obvious that both MVTT value and the mushy zone thickness go

together in relative proportion relationship. Results reveal that MVTT value does not put into effect the flow structure. Fine results are obtained with $dT = 5K$.

It should be emphasized here that MVTT was considered $dT = 5K$ viewing the numerical results relative to MVTT influence.

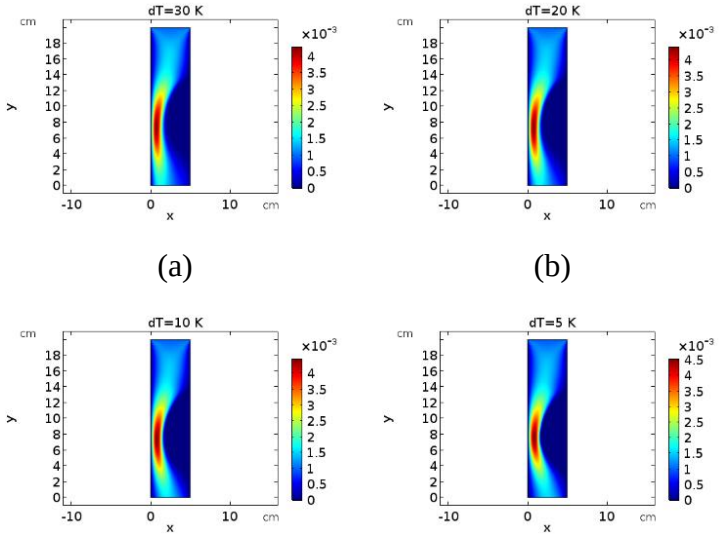

Fig.7. velocity field at different MVTT values ($v_0 = 0.001\mathrm{m/s}$ and time=200 s).

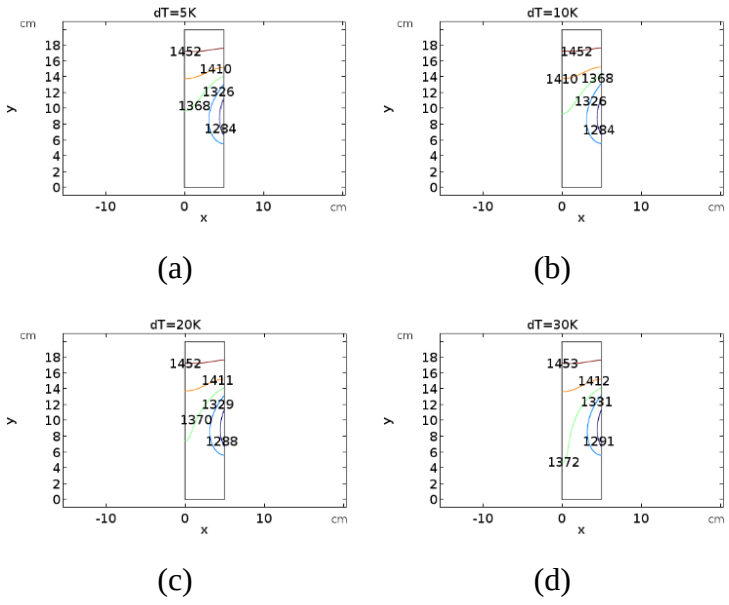

Fig.8. isothermal fields at different MVTT values ($v_0 = 0.001\mathrm{m/s}$ and time=200 s).

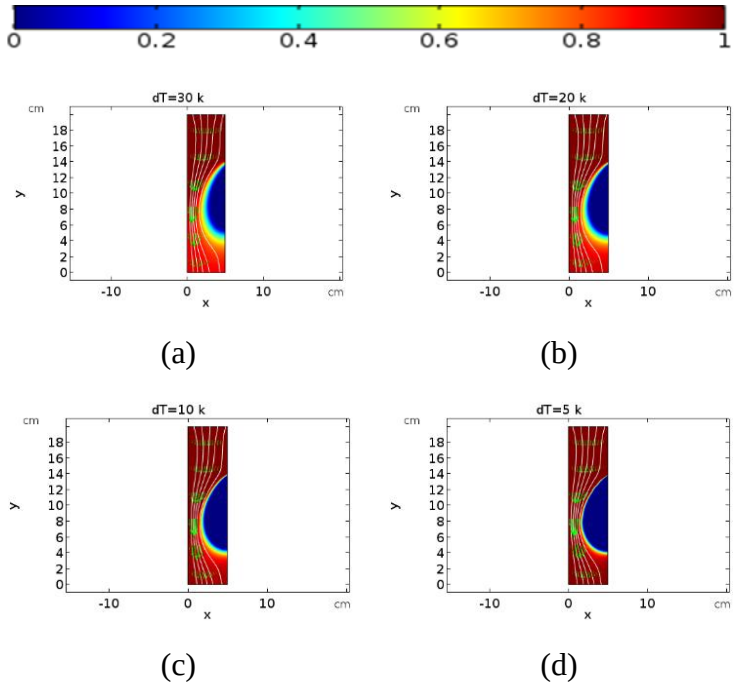

Fig.9. solid fraction and flow structure at different MVTT values ($v_0 = 0.001\,\mathrm{m/s}$ and time=200 s).

3.5 Effect of Flow Rate

3.5.1 Velocity Filed

Figure 10 shows the velocity fields and the impact of the flow rate on it for different inlet velocity conditions: (a) $v_0 = 0\,\mathrm{m/s}$, (b) $v_0 = 0.001\,\mathrm{m/s}$, (c) $v_0 = 0.002\,\mathrm{m/s}$ and (d) $v_0 = 0.005\,\mathrm{m/s}$ at same time step (200 s). Concerning case (a), results refer to stagnation in velocity all across the canal except for its entrance where a graduation in velocity spot can be distinguished with maximum value at its center (Fig. 7a). Unlike case (a) the rest of the cases (b)-(d) show a graduation in velocity across the canal taking its maximum value at the axial zone; noticing that the velocity goes faster in two cases: first near the walls just like in results found in case (d), second is while approaching to the solid area, which has seen in cases (b) and (c).

In cases (b), (c) and (d) forced convection phenomena was stronger than free convection, but in case (a) free convection influence is dominant due to inlet velocity condition which was set to be ($v_0 = 0\,\mathrm{m/s}$).

3.5.2 Temperature Filed

The impact of changing flow rate at same time step (200 s) on the isotherms is presented in Fig.11 ((a) $v_0 = 0\,\mathrm{m/s}$, (b) $v_0 = 0.001\,\mathrm{m/s}$, (c) $v_0 = 0.002\,\mathrm{m/s}$ and (d) $v_0 = 0.005\,\mathrm{m/s}$**)**. Results show that as the flow rate increases, the value of temperature increases as well beside cooled part; thus cooling rate decreases while raising the flow rate, the thing that make the process of solidification beside cooled part go in a decline matching what has been found in solid fraction result.

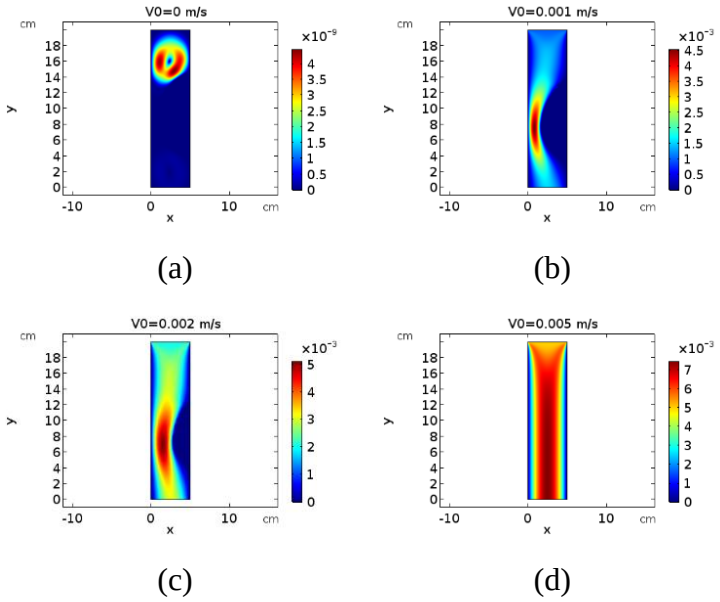

Fig.10. Velocity field at different flow rate ($dT = 5K$ and time=200 s).

3.5.3 Solid Fraction, Mushy Zone and Flow Structure

Figure 12 depicts the evolution of the solid fraction, mushy zone and flow structure at same time step (200 s) using different values of inlet velocity ((a) $v_0 = 0\,\mathrm{m/s}$, (b) $v_0 = 0.001\,\mathrm{m/s}$, (c) $v_0 = 0.002\,\mathrm{m/s}$ and (d) $v_0 = 0.005\,\mathrm{m/s}$**)**, or literally controlling the flow rate and as a result controlling both the spreading of the mushy zone and the development of solid state (phase). Results show that the intensity in the flow rate solid-state part decreases. The impact of the flow rate on the last income (d) is strong that the solid state cannot be observed during the process, i.e. there is an inverse relationship between the flow rate penetrating the canal and the solidification rate. In addition to the structure of the flow, an identical matching in solid area's shape and size is observed just like in cases (a), (b) and (c). Although, the flow

shape in both cases (a) and (d) is different. In case (a) with null set inlet velocity ($v_0 = 0\ \mathrm{m/s}$) the structure of the flow is shaped as a spiral, posing at the entrance part of the canal. In the same time, it is noticed that the flow structure took a regular shape from the entrance until exit of the canal in the case (d) because a solid area is not so obvious as in previous cases.

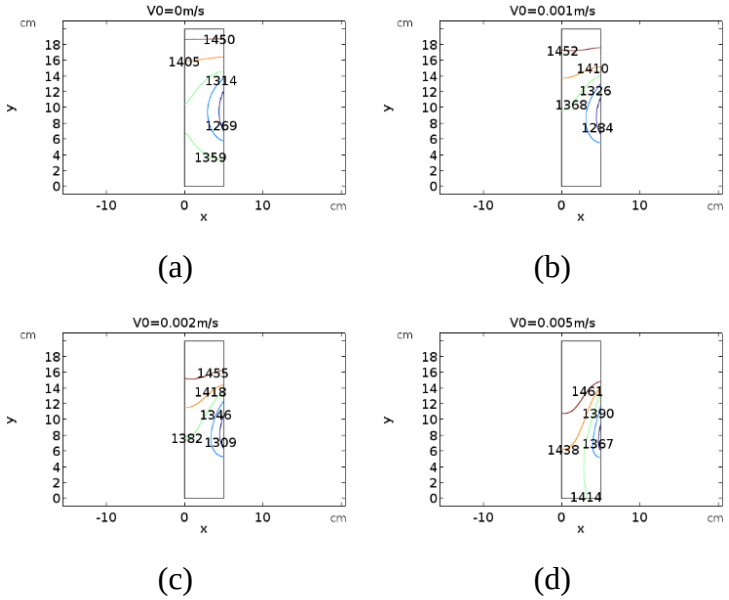

Fig.11. Isotherms at different flow rate ($dT = 5K$ and time=200 s).

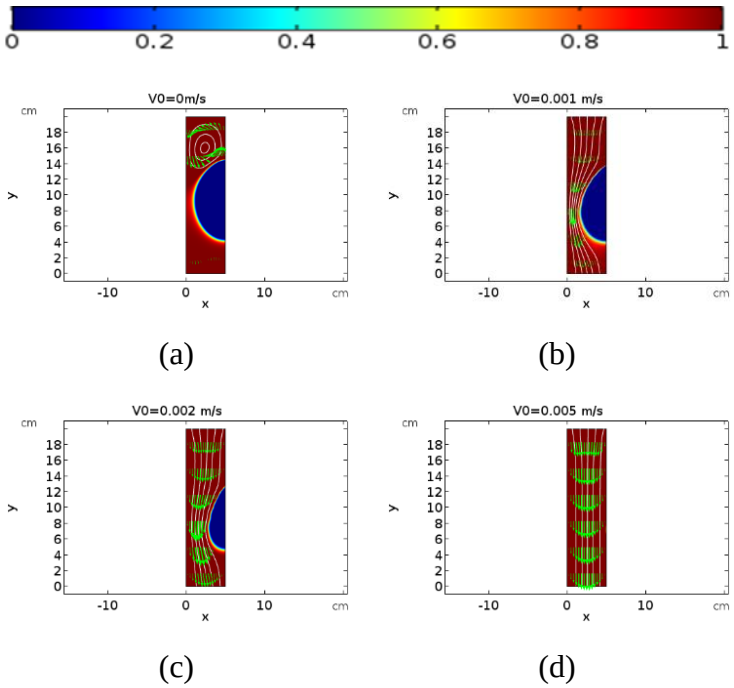

Fig.12. Solid fraction and flow structure at different flow rate ($dT = 5K$ and time=200s).

3.6 Suggested Different Cooling Rate Techniques

In this part, comparison is to establish between three different cases regarding the cooling process; the aim is to find the best among available ways, which can be used in actual applications such as molding, continue casting etc. The parameters of the comparison are the solidification rate and the development of the process, taking into account reducing the cooling process costs. The three ways (cases) formats are as follows: case (1): constant heat flux, $Q = -8\times10^5\ [\mathrm{W/m^2}]$, case (2): linear function heat flux, $Q = \left(-\frac{4\times10^5}{200[s]}t\right) - 4\times10^5[\mathrm{W/m^2}]$, and case (3): exponential function heat flux, $Q = -4\times10^5 e^{(t/200[s])}[\mathrm{W/m^2}]$. The melt flow velocity is set to be $v_0 = 0.001\mathrm{m/s}$.

Fig. 13 shows curves of the cooling heat flux development during the process.

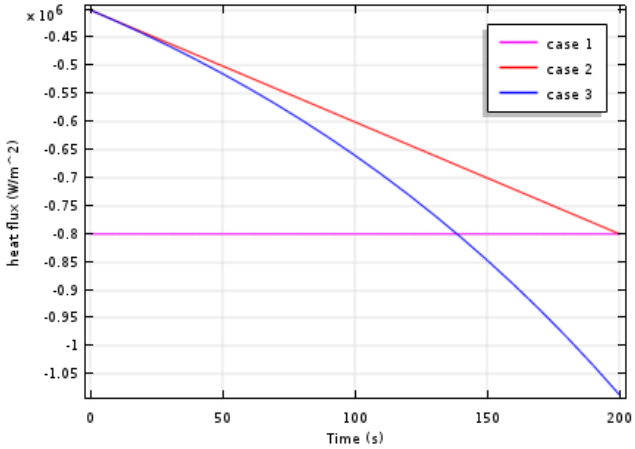

Fig.13. Heat flux variation.

3.6.1 Average of temperature on cold heat flux part

Figure 14 shows the average temperature history for different cases. The temperature drop in case one is faster in comparison to the other cases until it coincidences with second case's curve approximately at t= 170 s, and with third case's curve at t= 140s. After passing these two time steps the temperature drop dives slower in comparison to the other cases.

During the first 80 s of the process both case 2 and 3 are identical, then case 3 temperature drop goes faster than case 2; this is due to the fast development of the exp-function relative to case 3 flux (see Fig.13).

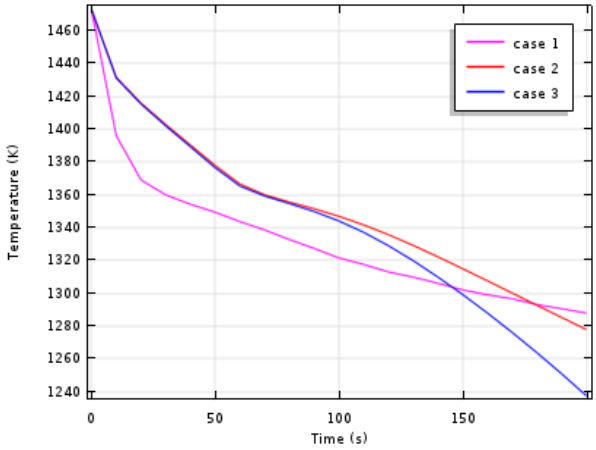

Fig.14. Average temperature

3.6.2 Solid Fraction Development for Different Cooling Parameters

The magenta, red and the blue curves express the average solid fraction time dependent development inside the canal of case 1, 2 and 3 respectively are presented in Fig.15. The solidification starts after 60 s in both cases 2 and 3 where it starts at 25 s in case 1.

It is obvious that the development rate increases with the time in each case as mentioned above (case 1, case 2 and case 3). Nevertheless, solid fraction values in case 1 go higher than the rest of the cases until it intersects with case 3 at t= 170 s approximately, and at t= 195 s approximately with case 2'curve. Right after the intersection, the solidification rate relative to case 1 becomes lower than the rest of the cases. Also, both curve 2, 3 are identical for the first 80 s because they share the same temperature profile as indicated in the discussion of Fig. 14.

The three cases' obtained results are plotted in fields (Fig.16) to support and get a review on the solid-melt development separated by the mushy zone for different time steps (t=50, 100 and 200s). At t= 50 s, it is clear that the solid part has only formed in case 1, and it becomes larger at t=100s in comparison to case 3 already bigger a bit than case 2. Although, it becomes wider in case 3 at t =200s in comparison to case 1 and 2. In addition, the solidified part in both cases 1 and 2 shares approximately the same size, hence, they match the same value at the end of process as indicated in curves Fig.15. Case 2 solidification rate is the lowest rate among other cases, but it converge into the same value relative to case 1 at t=195s approximately, this originated to the fact that case 2 cooling heat flux has reached the constant value of heat flux already used in case 1 $Q = -8\times10^{5}\ [\mathrm{W/m^2}]$ (see Fig.13).

The solid fraction in case 2 and 3 takes the same shape as an approximate half circle, but in case 1 it takes the shape of a drop, i.e. the solid part takes wider form in the left lower part. This may reflects the effect of the melting flow passing through the canal. Although, in case 2 and 3, the effect of the melt flow is weak. Using a melt flow in stagnation ($v_0 = 0\ \mathrm{m/s}$, see Fig.9) results in a solidified shaped spot similar to both case 2 and 3. Or it can be said that according to the late results once a time dependent cooling heat flux is applied the influence of the passing through melt flow fades remarkably (in the article by Wu *et al* [13]), hence the remelting is suppressed as well.

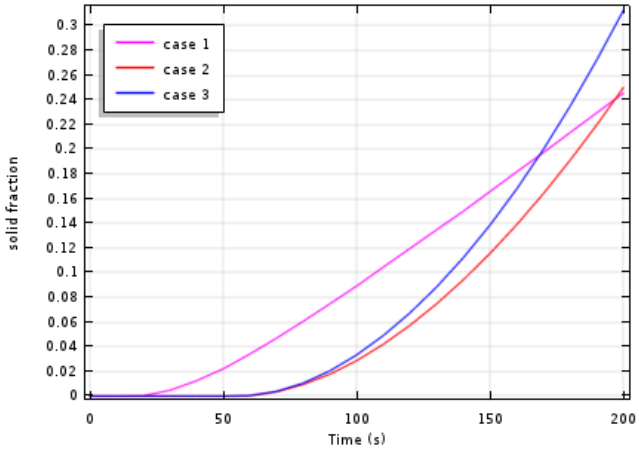

Fig.15. Average of solid fraction.

4. CONCLUSIONS

After results interpretation on the impact of MVTT, flow rate, and the comparison between apply two different cooling functions, which controlling the rate of cooling process to constant rate, the conclusions are listed as follow:

- Mushy zone got thicker when the MVTT value decreases and this is a mark of better numerical solution.
- Flow rate of the molten metal controlled by the inlet injected velocity inside the mold; affects on solidification rate, there is an inverse relationship between the melt flow and the solidification rate.
- Melt flow remelts the interface that has solidified immediately, due to the movement of the melt.

- Forced convection spread from the movement of the injected melt has stronger effect if compared to the free convection.
- Free convection is dominant and apparent just in case with null value of the inlet velocity (i.e., no exiting injected melt process).
- When a time variable linear heat flux is applied, the obtained solidification rate is quite the same as the one relative to the constant heat flux. Although, using linear heat flux eliminates the remelting phenomena, the fact that brings more economic benefits to the cooling process.

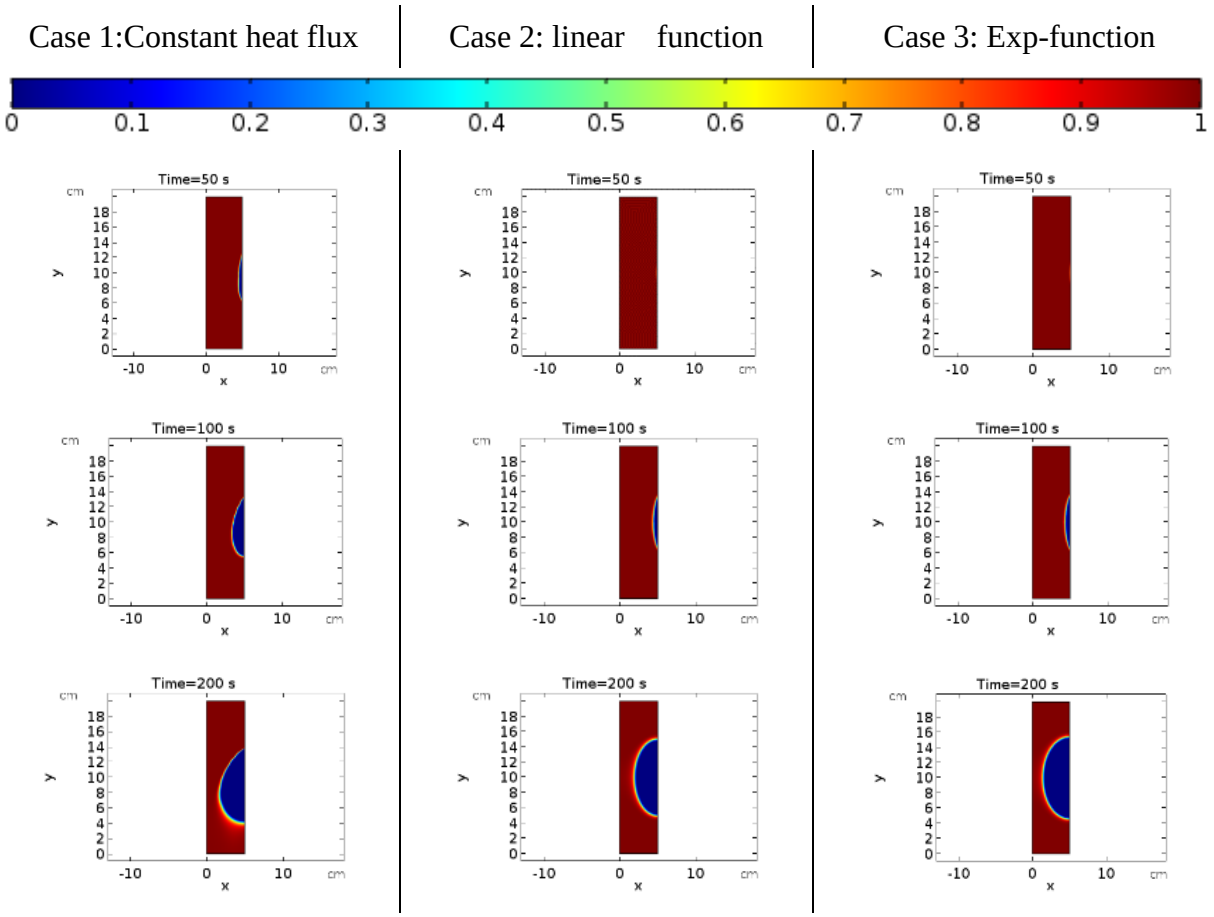

Fig.16. Solid fraction plots at different time steps ($v_0 = 0.001 m/s$ and $dT = 5K$).

5. NUMUCLATURE

Symbols

T temperature, K

p pressure, Nm^{-2}

k thermal conductivity, $W \cdot m^{-1} \cdot K^{-1}$

c_p Specific heat at constant pressure, J/kg.K

u superficial velocity, $m.s^{-1}$

v superficial velocity, $m.s^{-1}$

t time, s

v_0 inlet velocity, $m.s^{-1}$

f(T) enthalpy temperature function

H total enthalpy, kJ/kg

h sensible enthalpy, kJ/kg

ΔH Latent heat of fusion, kJ/kg

Q_{cooled} heat flux, $W \cdot m^{-2}$

Greek letters

β thermal expansion coefficient, K^{-1}

μ viscosity of the liquid, $N.s.m^{-2}$

ε_l porosity

ρ density, $kg.m^{-3}$

κ permeability, m^2

$\mathcal{A}$ porosity function

Exponents

l liquid

s solid

ref reference

6. REFERENCES

[1] Voller V. R, Prakash C. A fixed grid numerical modeling methodology for convection-diffusion mushy region phase-change problems. Int. J. Heat Mass Transfer. (1987). Vol.30, No.8. pp 1709-1719.

[2] Thomas B.G, O'Malley R. J, Shi T, Meng Y, Creech D, Stone D. Modeling of Casting. Welding and advanced solidification process IX, Aachen, Germany. 20-25 Aug. 2000. TMS. Warrendale, PA, 2000, pp. 769-76.

[3] Hussainy Ferhathullah S, Viquar Mohiuddin M, Laxminarayana P, Sundarrajan S. Solidification simulation of aluminum alloy casting – A theoretical and experimental approach. International Journal of Modern Engineering Research (IJMER). (2015). Vol. 5, Feb, pp. 1-10

[4] Hameed H, Mohammed A. A, Fadhil O. T. Effect of cooling intensity and position on solidification in semi-continuous casting of copper. Open Journal of Fluid Dynamics. 6, 182-197.

DOI: 10.4236/ojfd.2016. 63015

[5] Kirpo M. Global simulation of the Czochralski silicon crystal growth in ANSYS Fluent (2013), J. Cryst. Growth 371 60–69.

DOI: http://dx.doi.org/10.1016/j.jcrysgro.2013.02.005

[6] Sengupta J, B. Thomas G, and Wells M. A. Understanding the Role Water-cooling Plays during Continuous Casting of Steel and Aluminum Alloys. MS&T Conference Proceedings, (New Orleans, LA), AIST, Warrendale, PA (2004).

[7] Elliott A.J, Tin S, King W.T, Huang S.C, Gigliotti M.F.X, and Pollock T.M. Directional Solidification of Large Superalloy Castings with Radiation and Liquid-Metal Cooling: A Comparative Assessment. Metallurgical and materials transactions A, (2004), vol. 35A,

[8] Duan Q, Tan F.L, Leong K.C. A numerical study of solidification of n-hexadecane based on enthalpy formulation. Journal of materials processing technology. (2002).120 249–258.

DOI: 10.10161/S0924-0136(01)01188-8

[9] Rajesh Rajkolhe, Khan J. G. Defects, Causes and Their Remedies in Casting Process, International Journal of Research in Advent Technology. (2014). Vol.2, No.3

[10] Prabhakara Rao P, Chakraverthi G, Kumar A.C.S, Srinivasa Rao G. Modeling and Simulation of Solidification in Alloy Steel Sand Castings, International Journal of Thermal Technologies. (2011). Vol.1, No.1. pp.121-127

[11] ZHANG Xing-guo , ZHANG Wen-xiao , JIN Jun-ze , J. W. Evans. Flow of Steel in Mold Region During Continuous Casting. Interntional Journal of Iron and Steel Research, 2007, 14(2): 30-35, 41.

[12] Mahmoudi J. and Fredriksson H. An experimental and numerical study on the modelling of fluid flow. Heat transfer and solidification in a copper continuous strip casting process. Materials transactions. The Japan institute of metals. (2003).Vol. 44, No. 9 pp. 1741 to 1751.

[13] Wu M, Vakhrushev A, Nummer G, Pfeiler C, Kharicha A and Ludwig A. Importance of Melt Flow in Solidifying Mushy Zone. The Open Transport Phenomena Journal, (2010). 2, 16-23

[14] Frank P. Incropera , David P. Dewitt, Theodore L. Bergman, Adrienne S. Lavine. Fundamentals of heat and mas trandfer. JOHN WILEY & SONS, 2007, pp. 929

[15] Pantankar S. Y. Numerical heat transfer and fluid flow. Hemisphere. Washington. DC (1980).

[16] Carman P. C. Fluid flow through granular beds. Trans. Inst. Chem. Engs 15. 150-156. (1937).

DOI: 10.1016/S0263-8762(97)80003-2.

[17] Shmueli H, Ziskind G, Letan R. Melting in a vertical cylindrical tube: numerical investigation an comparison with experimentsInt. J. Heat Mass Transfer 53 4082-4091. (2010).

[18] Voller V. R, Cross M, Markatos N. C. An enthalpy method for convection/diffusion phase changes. Inr. J. Num. Meth. Engng 24, 221-284. (1987).

[19] Karunesh K, Shukla A, Atul S, Pascal H B. Melting and solidification behaviour of phase change materials with cyclic heating and cooling. Journal of Energy Storage 15 274–282. (2018).

[20] COMSOL Multiphysics User's Guide, Comsol, (2018). Http://www.comsol.com.

How to cite this article:
Bouzennada T, Mechighel F. Numerical study on the importance of the mixed convection and the impact of the cooling rate on the solidification of a pure material. J. Fundam. Appl. Sci., 2019, *11(3), 1188-1211*.